

## Rapid Laser-assisted Nanosizing Noble Silver Nanoparticles in Plant Extracts and Physiochemical Characterization

**Lamin S. Kassama, Ph.D**

Department of Food and Animal Sciences  
Carver Complex South RmA-101  
Alabama A and M. University  
4900 Meridian Street  
Normal, AL 35762

**Tatiana Kukhtareva**

Physics, Chemistry & Mathematics Department  
Alabama A&M University  
Normal, AL 35762

**Nickolai Kukhtarev**

Physics, Chemistry & Mathematics Department  
Alabama A&M University  
Normal, AL 35762

**Abiola John Kuponiyi**

Department of Food and Animal Sciences: A-101  
Alabama A and M. University  
4900 Meridian Street  
Normal, AL 35762

### Abstract

*Production of silver nanoparticles (AgNP) using different biological methods is gaining recognition due to their multiple applications. The objective of this study was to evaluate the effect of pulse laser application for rapid synthesis and homogeneous size reduction and distribution of nanoparticles. The extracts of Magnolia, Aloe Vera and Eucalyptus were used as reducing agents to produce the nanoparticles. During the pulse laser (Nd-YAG) illumination ( $\lambda=1064\&532\text{nm}$ ,  $PE=450\&200\text{mJ}$ , 10 Hz) the blue shift of the surface plasmon resonance absorption peak was observed at  $\sim 424$  to  $403\text{nm}$  range for AgNP. In addition, NNP solution after Nd-YAG illumination was characterized by the narrowing of the Surface Plasmon absorption resonance band which correlates to the monodispersity of the NNP distributions. FTIR, TEM, DLS, Zeta potential results demonstrated that NNP were surrounded by biological molecules which contributes to its natural stability.*

**Keywords:** Nanoparticles, laser, silver, Zeta Potential, FTIR, Plasmon, Differential light scattering, polydispersity

### Introduction

During the last decade various methods for Plasmon absorption resonance for the synthesis of nanoparticles, including micro emulsion techniques, organic-water-phase synthesis, and aqueous solution reduction were developed and investigated (Dadosh, 2009; Egorova & Revina, 2000; Pileni, 1997). In general, nanoparticles synthesis methods are divided into several groups: physical, chemical and biological techniques. In the case of physical synthesis, nanoparticles are assembled from atoms in the process of metal evaporation/condensation technique (Gurav, Kodas, Wang, Kauppinen, Joutsensaari, 1994). Generation of Nanoparticles (NP) using this technique has several disadvantages. Firstly, the tube furnace occupies large space, consumes high energy during the heating process, and takes long time to achieve thermal stability.

Another physical method for NP production is laser ablation of bulk metals in a solution (Mafune, Kohno, Takeda, & Kondow, 2003; Mafune, Kohno, Takeda, Kondow, & Sawabe, 2000, 2001). During the pulsed laser light illumination, NP sizes and shapes are modified due to the interaction with the laser light (Kazakevic, Simakin, Shafeev, BViau, Soumaref, & Bozon-Venduraz, 2007; Mafune et al., 2003; Samakin, Simakin, Shafeev, Soumaref, & Bozon-Venduraz, 2001; & Link, Burda, Nikoobakht, El-Sayed, 2000). The advantage of laser ablation compared to other conventional methods for preparing colloidal metal is the absence of chemical reagent in solution, which is important for some applications (Tsuji, Nakanishi, Mizuki, Tsuji, Doi, Yahiro, & Yamaki, 2009).

The physical methods are relatively complex processes and require sophisticated equipment and technologies; it consumes a great amount of energy. Hence, the chemical method of preparation NP is more widely used for stable colloidal nanoparticles preparation. The chemical method of NP synthesis are approached either in the classical or radiation methods. The classical approach uses the well-known chemical reducing substances (hydrazine, sodium borohydride, hydrogen, etc.), while the radiation-chemical process is initiated by solvated electrons generated by the ionizing radiation (Kholoud, Abou El-Nour, Ala'aEftaiha, Abdulrahman, Reda, & Ammar, 1998). The classical chemical techniques is subdivided into two categories: aqueous solutions with stabilizers and reverse micelles systems with aggregation processes. In the reverse micelles system, the growing NP are surrounded by surfactant molecules (Kaminskiene, Prosyfevas, Stonkute & Guobiene, 2013). The biosynthesis technique is similar to the chemical approach, but instead of toxic chemicals, biological components such as fungi, plant extracts, and bacteria are used. The green synthesis of nanoparticles has currently evolved into an important branch of nanotechnology (Prakash, Sharma, Ahmad, Ghosh & Sinha, 2011).

Syntheses of Noble-NP (NNP) have attracted many attentions (Daniel & Astruc, 2004; Sardar, Funston, Mulvaney, & Murray, 2009) because of their optical, catalytic and electrocatalytic properties, and high chemical stability. Noble-NP have potential application in surface-enhanced Raman Scattering (SERS) (Cao, Jin, & Mirkin, 2002); microelectronics (Kneipp, Wang, & Kneipp 1997; Kim, Roh, Kim, & Hong 2009; Wang, Hu, Lieber, & Sun, 2008), biolabeling, medical and diagnostic imaging (Tang, Fu, Lo, Hua, & Tuan, 2010; Huang, Neretina, & El-Sayed, 2009), X-ray contrast agents (Yoon, Choi, Kim, Kim, & 2007) and cancer therapy (Niidome, 2010; Wu, Ming, Wang, Wang, & Wang, 2010; Hunag et al., 2009; Huang, El-Sayed, Qian, El-Sayed, 2006). Because of their optical properties, studies on NNP are being actively conducted in various fields, including the study of chemical sensors (Rex, Hernandez, & Campiglia, 2006) and biosensors (Li, Luong, 2006) used for studying DNA or proteins.

Reaction kinetics provides valuable information on the formation of NNP using UV-Visible spectrophotometer (Okafor, 2013). Dynamic light scattering (DLS) technique is a non-invasive measuring of size of NNP in a dispersion. It measures the time-dependent fluctuations in the intensity of scattered light from suspension of particle undergoing random, Brownian motion. Particle size characterization of the hydrodynamic diameter of NNP was determined by Mewada, Pandley & Oza (2013). Characterization of biological compounds and its substituent groups were measured using Fourier Transform Infrared Spectroscopy (FTIR) by Rajendran, Natrajan, Siva Kumar, & Selvaraj (2010). The FTIR spectroscopy measures infrared intensity vs wavenumber of light. It provides information on the associated molecular profile of biochemical substances. This technique has been used to characterize AgNP synthesized with plant extracts and their associated molecular profile (Dur'an, Marcato, de Souza, Alves, & Esposito, 2007; Chandran, Chaudhary, Pasricha, Ahmad, & Sastry, 2006).

Silver nanoparticles (AgNP) are well known to possess antibacterial properties and microbial inhibitory potentials. Bacterial resistant to antibiotic poses serious challenges to food industry, regulatory agency and consumers alike. Therefore, there is need to control these problem in food system to enhance quality and food safety. Furthermore, significant economic loses were incurred by producers and public confidence eroding on poultry products. The need for an alternative technology to substitute antibiotic use cannot be overemphasized. Hence, the application Nano-engineered materials could provide a practical alternative to control microbial proliferation and promote food quality and safety. Hence, the objective of this research was to evaluate the effect of laser-assisted extracellular biosynthesis on the synthesized NNP.

## **Materials and Methods**

### **Sample Preparation**

Two-step approach is used in this experiment, the first step is the application of bio-photosynthesis approach for NNP using a biological (plant extracts) component as a reduction agent, and subsequently the application of pulse laser illumination to the bio-nano-solution. The extracellular biosynthesis of noble nanoparticles was accomplished using Magnolia (*Magnolia Grandiflora*), Eucalyptus (*Disambiguation*), and Aloe Vera (*Aloe barbadensis*) leaves water or ethanol extracts. The procedure of noble nanoparticles production was described in Okafor et al.(2013), thus synthesized with plant leaves extracts as a reducing agent for silver nitrate salt AgNO<sub>3</sub> (Carolina Biological Supplies).

### **Extraction Method of Biological Components**

Ten grams of leaves were washed and cut to fine sizes, boiled in 50mL of distilled sterilized water for 5 minutes, then 3mL of the filtrated plant /extract was added to a heated 75°C AgNO<sub>3</sub>solution (50mL -10–3M of AgNO<sub>3</sub>) as methods described by Kumar, & Yadav, 2009; Shankar, Ahmad, & Sastry (2003).The solution was then analyzed using the UV-Visible spectrophotometer (Cary 3E UV-Vis, Varian PTY Ltd. Australia). The finely cutplant leaves (10g) were extracted in 100 mL ethyl alcohol, C<sub>2</sub>O<sub>5</sub>OH, for 24 hours.

### **Biosynthesis and Characterization of AgNP's**

Approximately 3mL of the filtrated plant extract was added to a heated (75°C) AgNO<sub>3</sub> solution of 50mL of 10-3M of AgNO<sub>3</sub> (Kumar, & Yadav, 2009; Shankar, Ahmad, & Sastry, 2003).The reaction process was monitored using UV-Visible spectroscopy (Cary 3E UV-Vis, Varian PTY Ltd. Australia). The spectra of NNP solution was illuminated with a pulse laser (Surelite SL1-10,  $\lambda=1064$  nm, P = 450 mJ, 532nm,P=200mJ) at a pulse frequency of 10 Hz throughout the 20min process.

### **Physicochemical Characterization of AgNP's**

#### **Reaction Kinetics UV-Visible Spectrophotometer**

In the examination of NP, the complex optical property requires the understanding of the associated theories of laser light interaction with individual NP developed. For example, the measured absorbance spectrum does not show the actual absorbance but instead, shows the extinction of the light. The extinction is both the absorbed and the scattered light from the particles. Hence, the monitoring of the reaction was conducted in absorption mode with a UV-Visible spectroscopy(Cary 3E UV-Vis, Varian PTY Ltd. Australia).

#### **FTIR Profiling of Functional Groups**

Approximately 0.0016 grams of each NNP samples were dropped on FTIR card (Real Crystal IR Card, - 9.5 mm Aperture, International Crystal Labs, New Jersey, USA), as described by the method of Chandran (2006) protocol with some slight modifications. The infrared light passed through the samples and the continuing wave was captured by the detector connected to a computer (Thermo Fisher Scientific Smart Omni transmission, Madison, WI, USA) gives a sample spectrum. The result of analysis consisted of molecular binding form of certain functional group.

#### **Particle Size Distribution and Stability Measurements**

Differential light scattering (DLS) technique was used to determine the particle size distribution of the samples. The Zetasizer Nano Series (ZEN 3690, Malvern Instrument Ltd, Worcestershire, UK) is the premium system in the Zetasizer range. Two mL of the AgNP solutions were filled quartz cuvette for size characterization based intensity and volume and the Zeta cell for the determination zeta potential. Surface charges of AgNP were measured to determine the stability of NNP. Both measurements will be in accordance with the method described by White (2012).

## **Results and Discussion**

### **UV-Visible Spectroscopy**

The reaction of plants extract in the biosynthesis of NNP was monitored using UV-Visible spectroscopy. The kinetic of the reaction and the formation of AgNP using *Eucalyptus*-water-extract (EuWE) and *Eucalyptus*-ethanol-extract (EuEE) as a reduction agent is presented in Fig.1ab. The UV-Visible spectra of AgNPs solution illuminated with a pulse laser for the 20min period is shown in Fig. 2.

The monitoring of the reaction was conducted in UV-Spectroscopy absorption mode, hence the absorbance data was fitted to a Gaussian curve and the maximum peak was shown to occur at 437 nm for the AgNP formed with EuWE, while the absorption peak for EuEE is 417 nm.

The reaction kinetics shows the formation of stable nanoparticles in 25 min for EuWE and 20 min for EuEE. Higher AgNP concentration was obtained in EuEE in contrast to EuWE as shown in Fig. 1ab. The effect of laser illumination of AgNP shows drastic increase in concentration from highest absorbance index of about 0.65 (Fig. 1) to 3 shown in Fig. 2 after 40 & 50 min of post laser treatment. Thus, shows 4-fold increment of AgNP concentration for NPP synthesized with EuWE. Furthermore, improve homogeneity of the nanosolution was achieved as shown by the sharp absorption peak close to 400 nm (Fig. 2.), VonWhite II, Kerscher, Brown, Morella, McAllister, Dean, & Kitchens, (2012) reported an absorption peak of about 404 nm.

The NNP produced using *Aloe-Vera*-water-Extract (AVWE) and *Aloe-Vera*-ethanol-extracts (AVEE) are shown in Fig. 3ab. The maximum absorption peaks are obtained at 408 nm for both extracts and no significant increment of concentration as a result post-laser treatments was achieved with the AVWE (Fig.4.). Although, similar behavior was observed for NNPs solution produced using the *Magnolia-Grandiflora*-water-Extract (MGWE) and *Magnolia-Grandiflora*-water-ethanol-extracts (MGEE) under laser illumination. Post-laser treatment showed no significant increment of AgNP concentration for (MGWE), thus the absorption peak occurs at 421 and 420 nm as shown in Fig. 5, and similar kinetic trend of extracellular biosynthesis was reported by Okafor et al. (2013). Table 1 shows the hydrodynamic diameter of the three AgNP synthesized with the 3 plant extracts, ethanol extracts seem to give a better size compared to water extracts.

### Optical Characterization Nanosolution

Figure 6 shows the optical characterization of the NNP solution, and the increase color intensity was the result NNP concentration and UV-VIS absorbance (Fig. 1, 2, 3, 4, &5) are attributed to the increase in nanoparticle sizes. Absorbance measurements over time after synthesis showed no variation of optical density, suggesting that nucleation and growth occurs within the first 2-hour period. The change in color is indicative of size formation of NNP and aggregation as a result of laser illumination.

### FTIR Spectroscopy and TEM Experimental Results

The FTIR characterization of biological compounds and its substituent group profiles of the EuWE, EuEE, AVWE and AVEE are shown in Fig. 7. The result shows the nature of the stabilizing molecule in the formation of NPP, thus the information of the functional group of molecules. Figure 7 shows the comparison of the FTIR spectra of biosynthesized AgNP's before and after laser illumination. The spectra have slightly different behavior, but the main spectral peaks fall within the same wave numbers. Hence, laser illumination does not destroy the functional group of the stabilizing biological molecule but contributes to its structure. These results were corroborated by the TEM image shown in Fig. 8, which shows the nanoparticles are surrounded by a "film coat", which prevents nanoparticles from aggregation, thus indicative of stable NNP. The estimated size falls within 2-9nm range.

### DSL and Zeta Potential Measurements

The physical properties of the NNP are highly dependent on their sizes. Figure 9a depicts a plot of non-laser illuminated with two cluster molecules measured at high relative concentrations with hydrodynamic diameters of 6 and 60 nm. The polydispersity (two clusters) index improved to monodispersity (one cluster) with the hydrodynamic diameter of measures at 60 nm. The sizes of these samples were significantly larger than those determined with the TEM, this is because the TEM does not show sizes of the surface bio-molecular film coating of the NNP. The hydrodynamic size measurement using this method shows the average value, weighted by the particle scattering intensity. The measurement of the direct size of nanoparticles may not be appropriate, because the extracellular biosynthesis does not produce a pure NNP solution. Based on the results of the FTIR and TEM nanosolution can be defined as bio-Nanocomplexes. Unlike the TEM, the DLS technique is believed to measure bio-Nanocomplexes hence refereed as hydrodynamic diameter. The apparent Zeta potential provides information on the magnitude of the electrostatic charge repulsion or attraction between particles. This is one of the fundamental properties that are known to affect stability of nanosolutions. Figure 10ab showing results of the average value of Zeta potential -50 and -13.5 mV before and after laser illumination of nanosolutions for NNP with MGEE, respectively. The effect of post-laser illumination treatment increases the homogeneity of the NNP.

Figure 11abc shows transmission electron microscopy imaging of biosynthesized AgNP before and after laser irradiation. Large populations of small particles were observed in Fig. 11ab, which are spherical in shape. The accompanying large particle sintering leads to the formation of anisotropic structures, as evidence of multiple entangled particles shown in Fig. 11c. Chandran et al. (2006) also reported the slow reduction and crystallization causes the formation of multiple particles.

### Conclusion

Biosynthesis of NNP using plant (Eucalyptus, Magnolia and Aloe Vera) extract provides a simple and efficient mode of synthesis. The reaction kinetics shows the formation of stable NNP is accomplished within 60 min, shown with the zeta potential measurement ranging from -50 to -13.5 mV and the hydrodynamic sizes varied from 6 to 60 nm. The application of the pulsed laser illumination has proven to have impacted NNP concentration and size and size distributions and no severe effect on the substituent structures of the functional groups. FTIR techniques have shown that ethanol extract gave the best AgNP's with regards to particle sizes, functional group, rapid kinetics of reaction, higher concentration (ppm) and stability of particles. The FTIR, TEM, DLS, and Zeta potential results demonstrated that NNPs were surrounded by biological molecules, which naturally stabilized the nanosolutions.

### Acknowledgement

This work was supported by Evans Allen grant funded by USDA, the Title III Program of Alabama A&M University, and United States Department of Agriculture (USDA)-NIFA Capacity building grant and the Alabama A&M University Experimental Station.

### References

- Cao, Y. W. C., Jin, R. C. & Mirkin, C. A. (2002). Nanoparticles with Raman spectroscopic fingerprints for DNA and RNA detection. *Science* 297, 1536-40.
- Chandran, S.P., Chaudhary, M., Pasricha, R., Ahmad, A., Sastry, M. (2006). Synthesis of gold nanotriangles and silver nanoparticles using *Aloe vera* plant extract. *Biotechnol. Prog.*, 22, 577-583.
- Dadosh, T. (2009). Synthesis of uniform silver nanoparticles with a controllable size. *Material Lett.*, 63, 2236.
- Daniel, M.C. & Astruc, D. (2004). Gold nanoparticles: Assembly, supramolecular chemistry, quantum-size-related properties, and applications toward biology, catalysis, and nanotechnology. *Chem Rev*, 104, 293-346.
- Dur'an, N., Marcato, P. D., de Souza, G. I. H., Alves, O. L., & Esposito, E. "Antibacterial effect of silver nanoparticles produced by fungal process on textile fabrics and their effluent treatment," *Journal of Biomedical Nanotechnology*, 3(2), 203-208, 2007.
- Egorova, E. M. & Revina, A.A. (2000) Synthesis of metallic nanoparticles in reverse micelles in the presence of quercetin: *Colloids Surf. A: Physicochemical and Engineering Aspects*, 168, 87.
- Egorova, E.M. (2011) Interaction of silver nanoparticles with biological objects: antimicrobial properties and toxicity for the other living organisms, *Journal of Physics: Conference Series* 291.
- Gurav, A. S., Kodas, T. T., Wang, L.-M., Kauppinen, E. I. & Joutsensaari, J. (1994). Generation of nanometer-size fullerene particles via vapor condensation. *Chemical Physics Letters*, 218, 304-308.
- Huang, X. H., El-Sayed, I.H., Qian, W. & El-Sayed, M. A. (2006). Cancer cell imaging and photothermal therapy in the near-infrared region by using gold nanorods. *J Am Chem Soc* 128, 2115-20.
- Huang, X., Neretina, S. & El-Sayed, M. A. (2009). Gold nanorods: From synthesis and properties to biological and biomedical applications. *Adv Mater* 21, 4880-910.
- Kaminskiene, Z., Prosykevicius, I., Stonkute, J. & Guobiene, A. (2013). Evaluation of Optical Properties of Ag, Cu, and Co Nanoparticles Synthesized in Organic Medium. *Acta Physica Polonica a*, 23.
- Kazakevic, P., Simakin, A., Shafeev, G. G., Viau, G., Soumaref, Y. & Bozon-Verduraz, F. (2007). Laser-assisted shape selective fragmentation of nanoparticles. *Applied Surface Science*, 253, 7831-7834.
- Kholoud, M. M., El-Nour, A., Ala'a Eftaiha, Abdulrhman Al-Warthan, Reda & Ammar, A. A. (2010). Synthesis and applications of silver nanoparticles. *Arabian Journal of Chemistry*, 3 (3), 135-140.
- Kim, H.J., Roh, Y., Kim, S. K. & Hong, B. (2009). Fabrication and characterization of DNA-templated conductive gold nanoparticle chains. *J. Appl Phys*, 105, 074302.
- Kneipp, K., Wang Y., Kneipp, H. (1997), Single molecule detection using surface-enhanced Raman scattering (SERS). *Phys Rev Lett* 78, 1667-70.

- Kumar, V. & Yadav, S. K. (2009). Plant-mediated synthesis of silver and gold nanoparticles and their applications. *J Chem Technol Biotechnol.*, 84, 151–157.
- Li, C. Z. & Luong, J. H. T. (2006). Nanoparticles impedance sensing of DNA binding drugs using gold substrates modified with gold. WO2006021091.
- Link S., Burda, C., Nikoobakht, B., & El-Sayed, M. (2000). Laser-Induced Shape Changes of Colloidal Gold Nanorods Using Femtosecond and Nanosecond Laser Pulses, *Journal of Physical Chemistry B* 104, 6152
- Mafune, F., Kohno, J., Takeda, Y. & Kondow, T. (2003). Formation of stable platinum nanoparticles by laser ablation in water. *Journal of Physical Chemistry, B* 107, 4218, (2003)
- Mafune, F., Kohno, J., Takeda, Y., Kondow, T. & Sawabe, H. (2000). Formation of gold nanoparticles by laser ablation in water. *Journal of Physical Chemistry*, 104, 9111. .
- Mafune, F., Kohno, J., Takeda, Y., Kondow, T. & Sawabe, H. (2001). Formation of gold nanoparticles by laser ablation in aqueous solution of surfactant,” *Journal of Physical Chemistry. B* 105, 5114.
- Mewada, A., Pandey, S., & Oza, G. (2013) “A novel report on assessing pH dependent role of nitrate reductase on green biofabrication on gold nanoplates and nanocubes,” *Journal of Bionanoscience*, 7(2), 174–180.
- Niidome, T. (2010). Development of functional gold nanorods for bioimaging and photothermal therapy, *J. Phys: Conf Ser*, 232, 1-6.
- Okafor, F., Janen, A., Kukhtareva, T., Edwards, V. & Curley, M. (2013). Green Synthesis of Silver Nanoparticles, Their Characterization, Application and Antibacterial Activity. *Int. J. Environ. Res. Public Health*, doi:10.3390/ijerph90x000x,
- Pileni, M. P. (1997). Nanosized Particles Made in Colloidal Assemblies. *Langmuir*, 13, 3266.
- Prakash, A., Sharma, S., Ahmad, N., Ghosh, A. & Sinha, P. (2011). Synthesis of AgNPs by *Bacillus Cereus* Bacteria and Their Antimicrobial Potential. *Journal of Biomaterials and Nanobiotechnology*, 2, 156-162.
- Rex, M., Hernandez, F. E. & Campiglia, A. D. (2006). Pushing the limits of mercury sensors with gold nanorods. *Ann Chem*, 78, 445-51.
- Sardar, R., Funston, A. M., Mulvaney P., & Murray, R. W. (2009). Gold nanoparticles: Past, present, and future. *Langmuir* 25, 13840-51.
- Shankar, S. S., Ahmad, A., & Sastry, M. (2003). Geranium Leaf Assisted Biosynthesis of Silver Nanoparticles. *Biotechnol. Prog.*, 19, 1627-1631.
- Shankar, S.S., Rai, A., Ahmad, A. & Sastry, M. (2005). Controlling the optical properties of lemongrass extract synthesized gold nanotriangles and potential application in infrared-absorbing optical coatings. *Chem Mater.*, 17(3), 566–572.
- Simakin, A. V., Voronov, V. V., Shafeev, G. A., Brayner, R. R., & Bozon-Verduraz F. (2001). Nanodisk of Au and Ag produced by laser ablation in liquid environment. *Chem. Phys. Lett.*, 348, 182.
- Tang, S. C., Fu, Y. Y., Lo, W. F., Hua, T. E. & Tuan, H. Y. (2010). Vascular labeling of luminescent gold nanorods enables 3-D microscopy of mouse intestinal capillaries. *ACS Nano*, 4, 6278-84.
- Tsuji, T., Nakanishi, M., Mizuki, T., Tsuji, M., Doi, T., Yahiro, T. & Yamaki, J. (2009). Preparation of nano-sized functional materials using laser ablation in liquids. *Applied Surface Science* 255, 9626–9629.
- VonWhite II, G., Kerscher, P., Brown, R., Morella, J. D., McAllister, W., Dean, D., & Kitchens, C. L. (2012). Green Synthesis of Robust, Biocompatible Silver Nanoparticles Using Garlic Extract. *Journal of Nanomaterials*, 1-12.
- Wang C., Hu, Y. J., Lieber, C. M., & Sun, S. H. (2008). Ultrathin Au nanowires and their transport properties. *J. Am Chem Soc* 130: 8902-3.
- White, G., Kerscher, P., Brown, R., Morella, J., McAllister, W., Dean, D., & Kitchens, C. (2012). Green Synthesis of Robust, Biocompatible Silver Nanoparticles Using Garlic Extract. *Journal of Nanomaterials*, 1-12.
- Wu, X., Ming, T., Wang, X., Wang, P., Wang, J., & Chen, J. (2010). High photoluminescence-yield gold nanocubes: For cell imaging and photothermal therapy. *ACS Nano*, 4, 113-120.
- Yoon, K.H., Choi, K., Kim S. & Kim, S. (2007). X-ray contrast agent using gold nanoparticles and process for preparing the same. WO2007129791.

**Table 1: The average value of the hydrodynamic diameter (Dia nm) and the surface Plasmon absorption resonance peak ( $\lambda$  nm) before and after laser illumination of AgNP nanosolution with Eucalyptus, Magnolia and Aloe Vera Extracts**

Treatment	Hydrodynamic diameter (Dia. (nm)) & Plasmon absorption Peak ( $\lambda$ (nm))											
	Eucalyptus				Magnolia				Aloe Vera			
	$\lambda$ (nm)		Dia (nm)		$\lambda$ (nm)		Dia (nm)		$\lambda$ (nm)		Dia (nm)	
No-Illumination	Eth	H <sub>2</sub> O	Eth	H <sub>2</sub> O	Eth	H <sub>2</sub> O	Eth	H <sub>2</sub> O	Eth	H <sub>2</sub> O	Eth	H <sub>2</sub> O
Illumination	426	426	29	35	420	421	33	48	424	-	70	-
Illumination	408	409	52	62	414	411	54	71	418	-	64	-

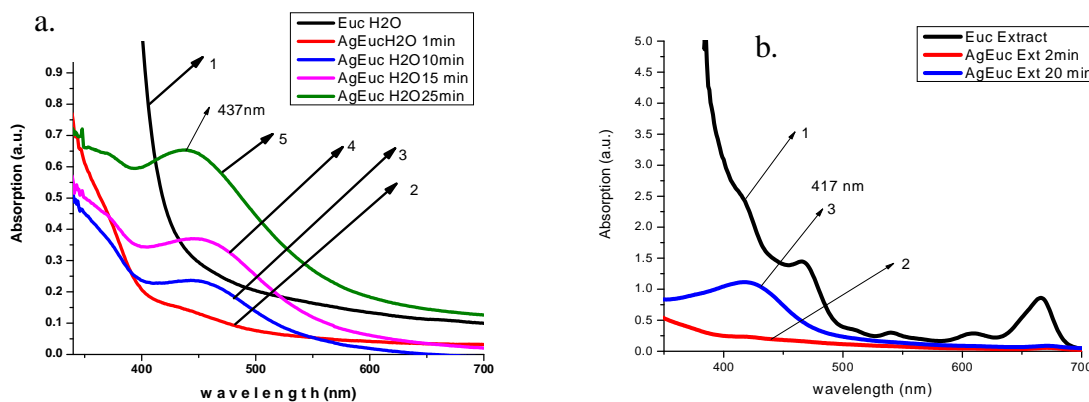


**Fig.1. Kinetic of reaction process of AgNP production using (a) Eucalyptus H<sub>2</sub>O extract, and (b) Eucalyptus Ethanol extract: Curve label 1 reaction time 0 min, 2 reaction time of 1 min and 2 min for ethanol, 3. Reaction time of 10 min and 20 min for ethanol, and 4. Reaction time of 15 min**

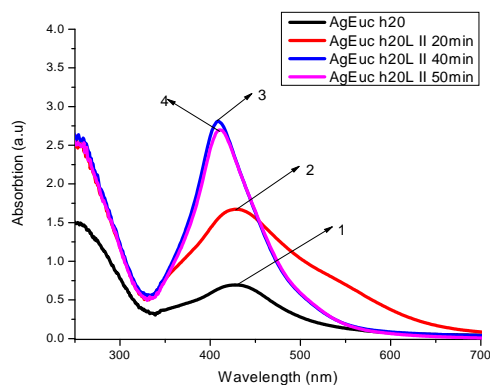


**Fig.2: UV-Visible spectra of AgNP solution reduced using *Eucalyptus* water extract after laser illumination: Curve label 1 extracellular biosynthesized no-laser illumination, 2. laser illumination for 20 min, 3. 40 min, and 4.50 min.**

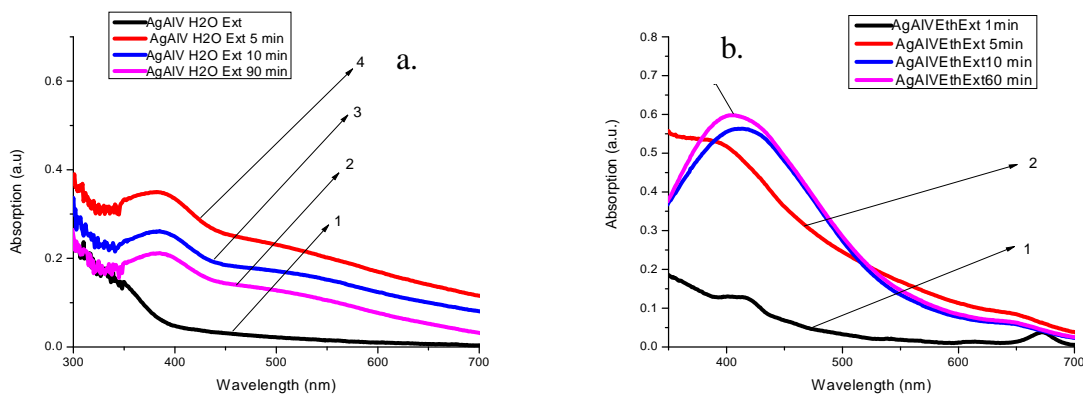


**Fig. 3. Kinetic of reaction process of the AgNP nanosolution (a) *Aloe vera*H<sub>2</sub>O extract, (b) *Aloe vera*Ethanol extract. Curve label 1. Reaction time of 0 min water extract and 1 min for ethanol extract; 2. Reaction time of 5 min for both; 3. Reaction time of 10 min for both; 4. Reaction time of 90 min for water and 60 min for Ethanol extract**

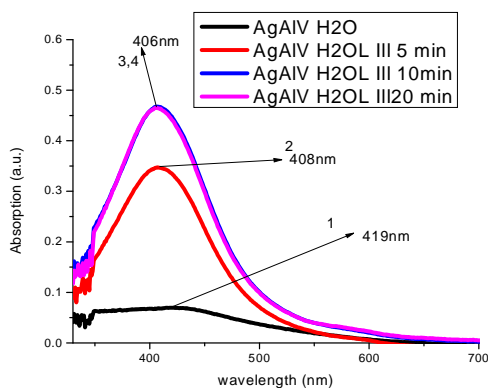


**Fig.4. UV-Visible spectra of AgNP (a) *Aloe vera*H<sub>2</sub>O extract: curve label 1. No-laser illumination, 2 laser illumination for 5 min, 3. laser illumination for 10 min, and 4. laser illumination for 10 min.**

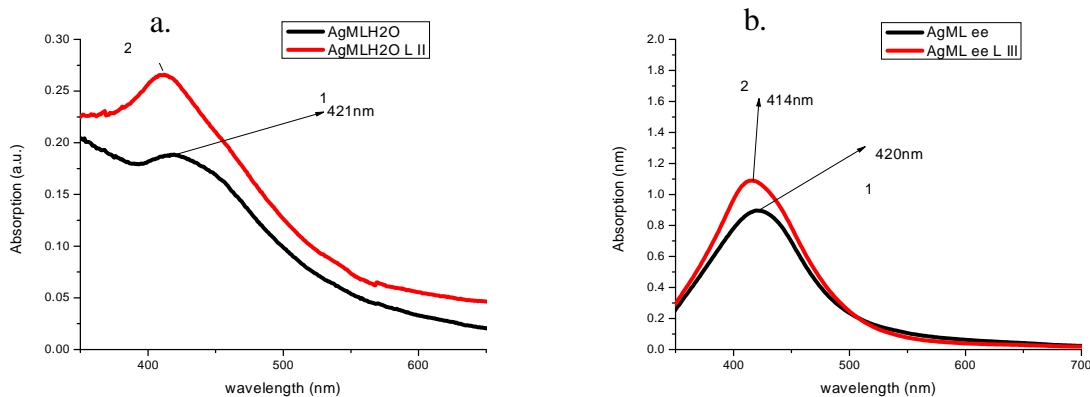


**Fig. 5. UV-Visible spectra of AgNP's produced Magnolia Grandiflora(a) water extract and (b) ethanol extract: curve label 1. No-laser illumination, 2.laser illumination for 20 min**





Fig.6. Visual appearance of the biosynthesized AgNP nanosolution: (1) after laser illumination, (2) before laser illumination

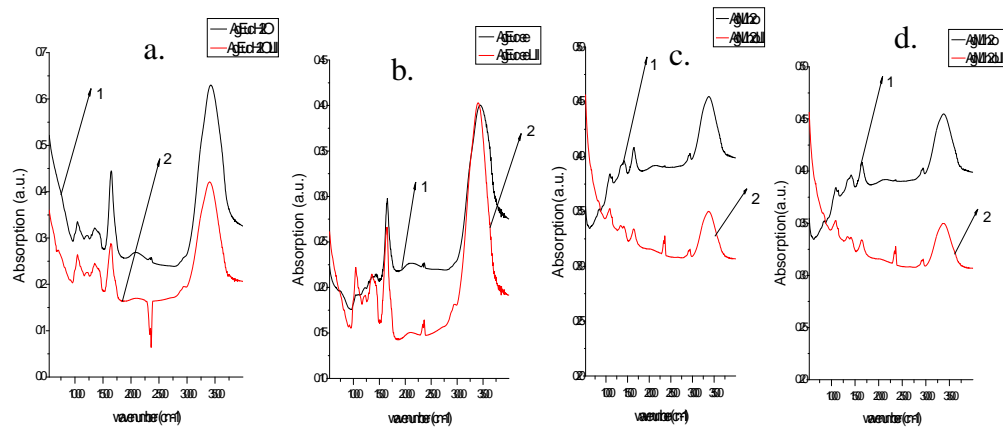


Fig.7: FTIR spectra of biosynthesized AgNPnanosolution (a) EuWE, (b) EuEE, (c) AVWE, and (d) AVEE. Curve label 1is nanosolution before laser illumination, and 2. afterlaser illumination.

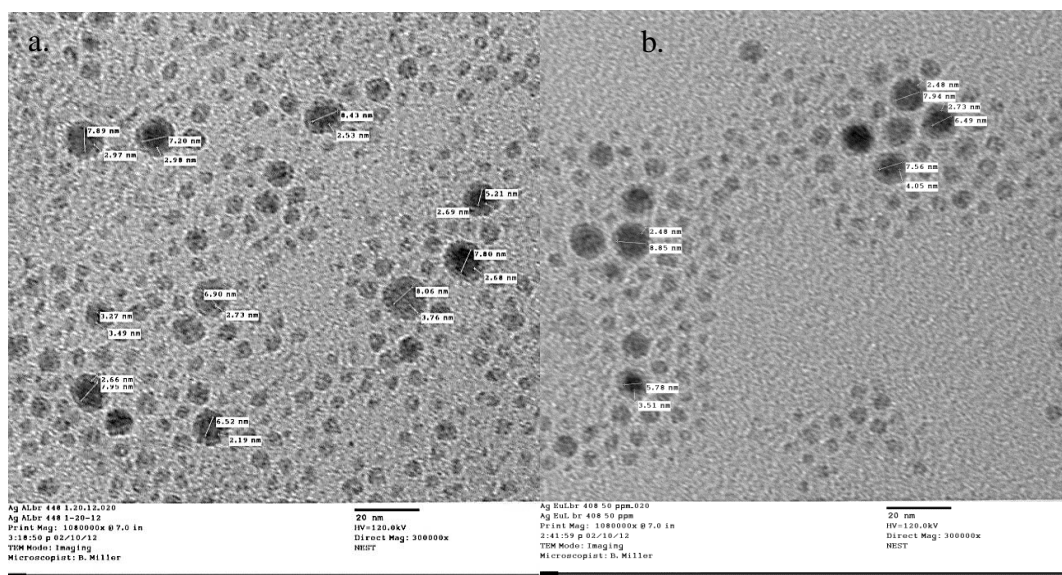


Fig. 8. Transmission Electron Microscopy Images of AgNP Aloe Vera (a) and Eucalyptus (b) after laser illumination ay 20nm scale range.

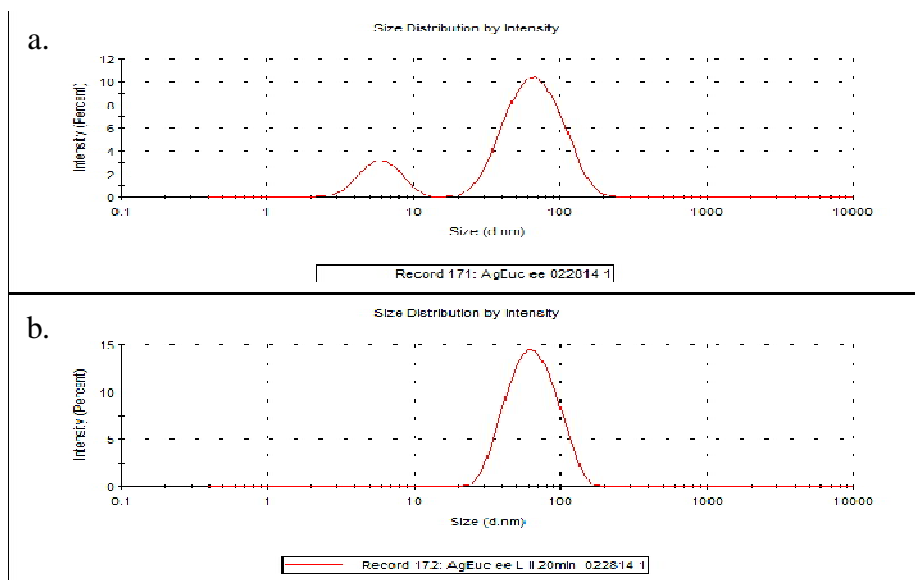


Fig.9: Size distribution of AgNP EuEE by intensity (a) before illumination and (b) after illumination

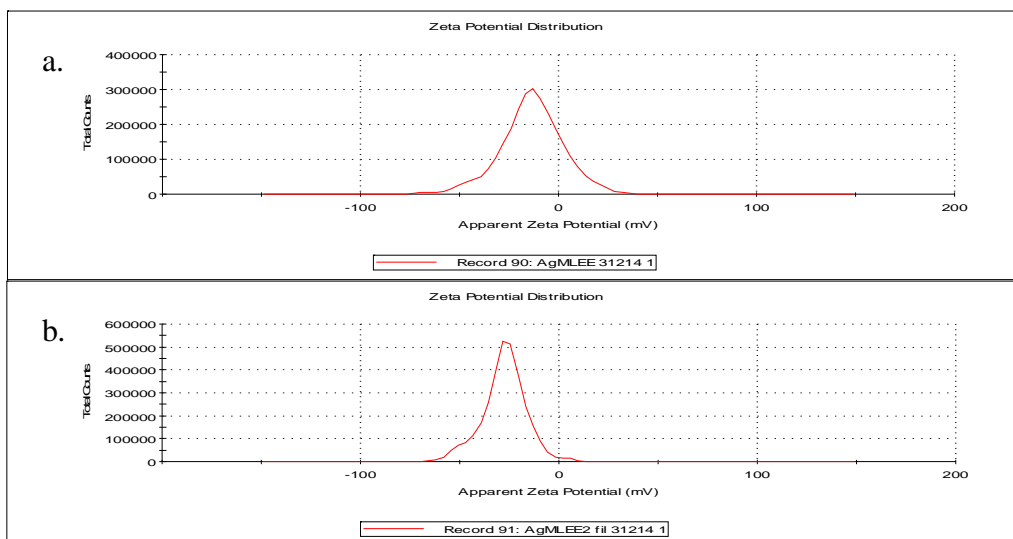
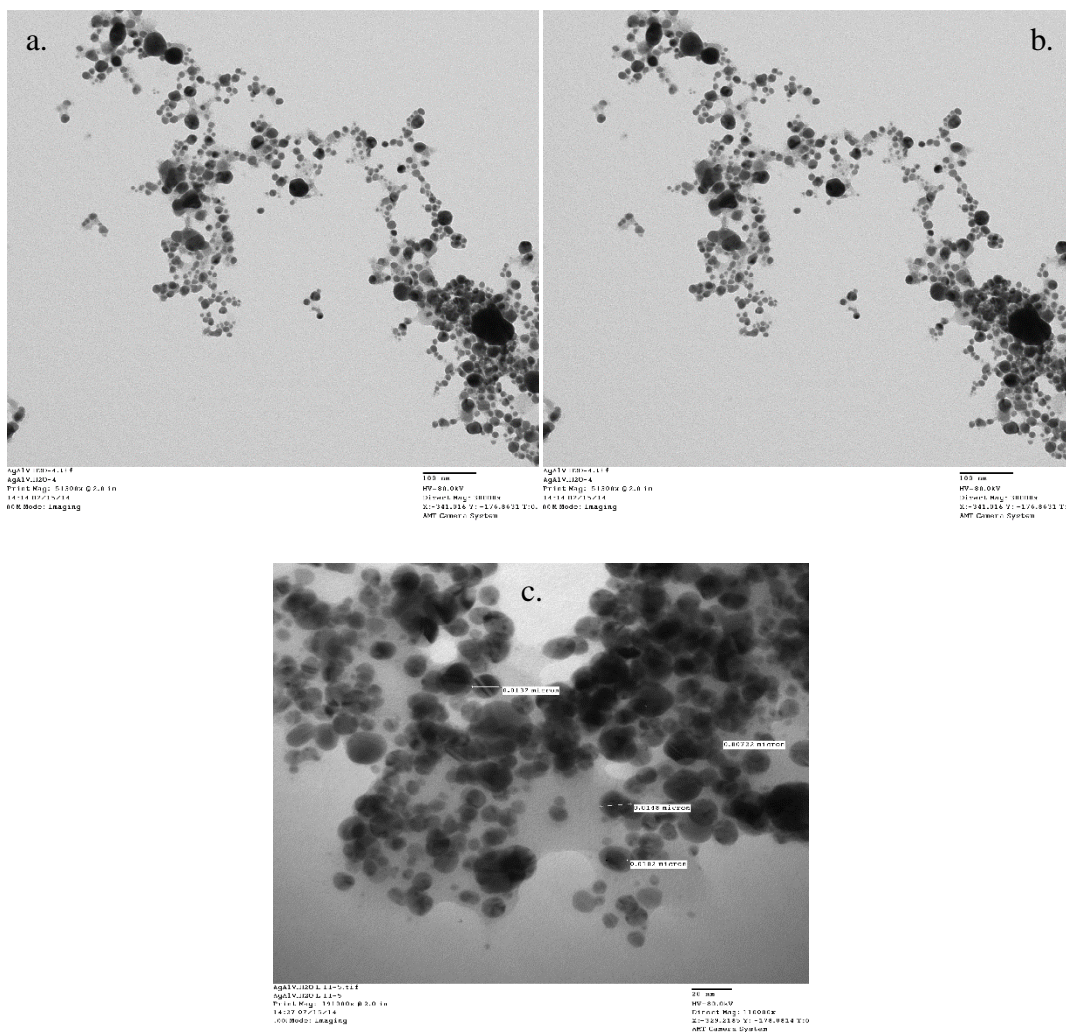


Fig.10. Zeta potential distribution of AgNP MGEE (a) before laser illumination and (b) after laser illumination



**Fig.11. Transmission Electron Microscopy Images of AgNP (a) before laser, (b) after laser illumination (bar -100nm, (c) – 20nm**